Transpiration drives diurnal and seasonal streamflow in secondary tropical montane forests of Eastern Himalaya

Manish Kumar[1], Yangchenla Bhutia[2], Gladwin Joseph[3], and Jagdish Krishnaswamy[2]

[1]University of Birmingham Edgbaston Campus
[2]Ashoka Trust for Research in Ecology and the Environment
[3]Conservation Biology Institute

December 8, 2022

Abstract

Vegetation studies establishing direct mechanistic linkages between stand transpiration and streamflow are rare from sub-tropical and tropical montane forests (TMFs) like Himalaya. We quantified the impact of diurnal and seasonal transpiration on lean season streamflow in a broad-leaved evergreen secondary TMF in Eastern Himalaya. Whole-tree and stand transpiration were measured using Granier's thermal dissipiation sap flow probes at one of the wettest (4500 mm yr-1) and highest elevation (2100 m) sites in the world to date. The observed daily and annual transpiration rates were double of the reported values from TMFs in relatively drier Central Himalaya, but at the lower bound of TMFs globally. Solar radiation was the key driver of transpiration in energy-limited winter under hydrated conditions. Vapour pressure deficit (D) controlled transpiration in energy-abundant summer. We also found that moderate precipitation events (10-30 mm) followed by clear skies can induce significant increase (93±110 %) in stand transpiration. In turn, transpiration was the main driver of lean season streamflow in dry winter and to a lesser extent in wet summer. Thus, in winter, the transpiration-driven abstraction induced corresponding diurnal cycles in soil moisture and streamflow with an average lag of 1.3±1.8 hours and 2.9±2.5 hours, respectively, and strong negative correlations (-0.8±0.1). Thus, changes in vegetation cover and precipitation patterns are likely to impact local and regional moisture recycling by vegetation and lean season flow, thereby affecting regional water security in the Eastern Himalaya.

Manuscript Title:

Transpiration drives diurnal and seasonal streamflow in secondary tropical montane forests of Eastern Himalaya

Authors:

Manish Kumar[a,b,c*], Yangchenla Bhutia[b,c,d], Gladwin Joseph[b,c,e] and Jagdish Krishnaswamy[b,c,f]

Affiliations:

[a]School of Geography, Earth and Environmental Sciences, University of Birmingham, Edgbaston, Birmingham, B15 2TT, United Kingdom.

[b]Ashoka Trust for Research in Ecology and the Environment (ATREE), Royal enclave, Srirampura, Jakkur PO, Bangalore 560064, Karnataka, India.

[c]Manipal Academy of Higher Education (MAHE), Manipal 576104, Karnataka, India.

[d]Sikkim State Council of Science & Technology, Gangtok 737102, India.

[e]Conservation Biology Institute, Oregon 97333, USA.

[f]School of Environment and Sustainability, Indian Institute for Human Settlements, Bangalore 560080, India.

*Corresponding author: Manish Kumar

Corresponding author contact information

Dr. Manish Kumar

Research Fellow,

School of Geography, Earth and Environmental Sciences

University of Birmingham, Edgbaston, Birmingham, B15 2TT, United Kingdom

Mobile: +44 7927645279

Primary email id: manish.kumar@atree.org ; m.kumar.2@bham.ac.uk

ORCID: 0000-0002-6780-9336

Running head

Transpiration drives dry season streamflow in secondary Eastern Himalayan Forests

Keywords

Eastern Himalaya; Ecohydrology; Plant-water relations; Sap flow; Secondary forests; Streamflow; Transpiration; Tropical montane forests

Abstract

Vegetation studies establishing direct mechanistic linkages between stand transpiration and streamflow are rare from sub-tropical and tropical montane forests (TMFs) like Himalaya. We quantified the impact of diurnal and seasonal transpiration on lean season streamflow in a broad-leaved evergreen secondary TMF in Eastern Himalaya. Whole-tree and stand transpiration were measured using Granier's thermal dissipiation sap flow probes at one of the wettest (4500 mm yr^{-1}) and highest elevation (2100 m) sites in the world to date. The observed daily and annual transpiration rates were double of the reported values from TMFs in relatively drier Central Himalaya, but at the lower bound of TMFs globally. Solar radiation was the key driver of transpiration in energy-limited winter under hydrated conditions. Vapour pressure deficit (D) controlled transpiration in energy-abundant summer. We also found that moderate precipitation events (10-30 mm) followed by clear skies can induce significant increase (93±110 %) in stand transpiration. In turn, transpiration was the main driver of lean season streamflow in dry winter and to a lesser extent in wet summer. Thus, in winter, the transpiration-driven abstraction induced corresponding diurnal cycles in soil moisture and streamflow with an average lag of 1.3±1.8 hours and 2.9±2.5 hours, respectively, and strong negative correlations (-0.8±0.1). Thus, changes in vegetation cover and precipitation patterns are likely to impact local and regional moisture recycling by vegetation and lean season flow, thereby affecting regional water security in the Eastern Himalaya.

Graphical Abstract

[Insert Graphical Abstract]

1. INTRODUCTION

Moisture recycling by vegetation is a key ecohydrological process in tropical forest hydrology (Wohl *et al.* , 2012). While, the impact of climate regimes on the evolution of distinct vegetation types is well known, vegetation also significantly alters the availability of water in their environment through ecohydrological processes such as transpiration and infiltration of precipitation into the soil (Peña-Arancibia *et al.* , 2019). These two processes modulate soil moisture distribution across both time and at local and regional scales,

and significantly influence hydrological services from vegetated catchments such as streamflow (Bruijnzeel, 2004; Schlesinger and Jasechko, 2014). The extent of vegetative influence on streamflow varies considerably across vegetation types, dominant functional groups, micro-climatic conditions (water or energy-limitations on plant productivity) and the ability of vegetation to access deeper subsurface moisture and/or groundwater. The literature on interactions between water and vegetation has been largely focused on the ecophysiological aspects of transpiration, while a few have extended it to interactions between transpiration, subsurface moisture, and streamflow (Bond*et al.* , 2002; Moore *et al.* , 2011). In terrestrial ecosystems, diurnal and seasonal variations in transpiration can induce corresponding patterns in soil moisture and streamflow (Bond *et al.* , 2002; Moore *et al.* , 2011). Conversely, the transpiration responses to changes in antecedent moisture and precipitation pulses is another emerging area of research, especially in regions with extended dry spells (Burgess, 2006; Zeppel*et al.* , 2008; Chen *et al.* , 2014).

Ecohydrological studies have explored the relative impact of transpiration on hydrological fluxes at different spatiotemporal scales and across different functional groups (Asbjornsen *et al.* , 2011). For example, shallow-rooted trees may tap into the subsurface moisture, whereas deep-rooted tree species can access the water table directly, and releases it into the atmosphere through transpiration (Maeght *et al.* , 2013; Kumar *et al.* , 2022). Deng *et al.* , (2021) report groundwater table modulating sap flow in karst aquifer systems, along with meteorological drivers. The loss of soil moisture or baseflow to the atmosphere, which otherwise could have contributed to streamflow, can significantly alter the local water balance and hydrological services from a forest (Barbeta and Peñuelas, 2017; Perry and Jones, 2017). In contrast, the "two water worlds" hypothesis suggests that the water available for trees is potentially disconnected from the moisture stock that contributes to streamflow and that trees have limited access to groundwater (Berry *et al.* , 2018). However, the literature remains inconclusive on the presence of two moisture movement pathways with research evidence on trees accessing stream/groundwater in the valley or riparian zones, especially in topical montane forests (TMFs) with shallow soil strata, highly fractured geology, and significant dry season as seen in the Himalaya and Western Ghats of India (Krishnaswamy *et al.* , 2013; Barbeta and Peñuelas, 2017). However, the literature on interlinkages between vegetation and streamflow remains scarce from pan-tropical mountains such as Himalaya (Célleri and Feyen, 2009; Bruijnzeel *et al.* , 2011).

Previous research from Himalaya does highlight the important role of broad-leaved TMFs in precipitation partitioning, runoff generation, and sediment transport in the Himalaya, where evapotranspiration can go up to 40 % of the annual water budget (Sharma *et al.* , 2007; Ghimire *et al.* , 2014; Qazi *et al.* , 2017). At basin scales, studies on stream hydrology have tried to understand the relative contribution of glacial melt, snowmelt, runoff, and baseflow to the total discharge and quantify the impact of climate change in Himalaya (Singh and Bengtsson, 2005; Singh and Kumar, 2010). At catchment scales, most of such studies have come from the Western and Central (Nepal) Himalaya and have focused on establishing linkages between stream characteristics and land-use forms, including the role of TMFs (Sharma *et al.* , 2007; Krishnaswamy, 2017). The region is projected to experience significant warming (0.8-1.2 °C decade^{-1}), increasingly drier winters and wetter monsoon and summer seasons trends under climate change (Krishnan *et al.* , 2019; Kumar *et al.* , 2021). Broad-leaved secondary forests form a significant portion (32.5 %) of total area under TMFs in Sikkim and are likely to have distinctly altered carbon and water cycles than primary forests (Kanade and John, 2018; Bhutia *et al.* , 2019). The high water demand from these regenerating secondary forests dominated by pioneer species can exert significant pressures on limited soil moisture reserves and in turn on lean season streamflows (Wright *et al.* , 2018; Kumar *et al.* , 2022). However, to the best of our knowledge, ecohydrological controls of vegetation-water use on streamflow have not been quantified and mechanistically explained in TMFs of Himalaya. Thus, in the first attempt from Himalaya, the relative controls of vegetation-driven transpiration on lean season streamflow were investigated in Sikkim, a representative region of Eastern Himalaya. Thus, the key questions addressed in the study are: (a) How does micro-climate and soil moisture changes affect diurnal and seasonal variability in stand transpiration?, (b) What is the impact of precipitation events size on stand transpiration?, and (c) How diurnal and seasonal variability in stand transpiration impacts lean season streamflow dynamics in an East Himalayan secondary TMF?

2. MATERIAL AND METHODS

2.1. Study site and forest stand description

The study site is located in the Fambong-Lho Wildlife sanctuary (FWS, N27.583, E88.933) draining into Teesta river) in East Sikkim, which is part of the Teesta river basin (Figure 1). The instrumented micro-watershed has a catchment area of 0.016 km^2 and is situated at an elevation of 2100 - 2400 meters above sea level (masl). The mean annual precipitation is 4650±120 mm with temperature fluctuating between an annual maximum of 240C to minima of -20C. Three distinct seasons in the study area are winter (November - February) with sunny days, freezing nights, sporadic snowfall and low evapotranspiration, summer (March-May) characterized by warm and cloudy days, high evapotranspiration, and substantial pre-monsoon precipitation, and monsoon (June - October) with high humidity, low evapotranspiration and concentrated precipitation (Pandey *et al.* , 2016; Kumar *et al.* , 2021). The winter (December 2013 – February 2014) marked the dry season with sunny but cold days and sub-zero night temperatures. The summer (March 2014 – May 2014) saw increased day-length, predominantly afternoon precipitation, abundant moisture, warmer temperatures, and higher plant productivity (Kumar *et al.* , 2022).

[Insert Figure 1]

Figure 1. Study area map showing (a) Digital elevation model (DEM) map of Himalaya and Sikkim within India; (b) the location of Fambong-Lho wildlife sanctuary (FWS) and the instrumented watershed within Sikkim; and (c) DEM of the delineated watershed of the first-order stream in FWS with the location of the sap flow instrumentation site, and rain and stream gauging stations.

The forest soil was well-drained sandy-loam with an average soil depth of 70 cm. The stand was moderately sloped (10°-35°) and dominated by north-east aspect. The site showed much lower soil hydraulic conductivity than similar elevation forests in Central Himalaya, a known characteristic of secondary forests (Wright *et al.* , 2018). The forest stand represents early successional secondary East Himalayan broad-leaved wet montane forests (Sudhakar *et al.* , 2008; Kanade and John, 2018) and as a mid-altitude forests dominated by*Castanopsis hystrix* (Bhutia *et al.* , 2019). The stand is characterized by (a) the dominance of broad-leaved evergreen species and (b) sub-tropical montane climate with high precipitation and strong diurnal and seasonal temperature gradients. The vegetation data were derived from five 1000 m^2 (100 m X 10 m) vegetation survey plots (Bhutia *et al.* , 2019). The species composition is dominated by the three species: *Symplocos racemosa* , *Eurya acuminata,* and *Castanopsis hystrix* , which form 58.3 % of total stand trees and 38.3 % of the total basal area (Bhutia *et al.* , 2019; Kumar *et al.* , 2022). The short-statured canopy (3-8 m tall) is dominated by pioneer species like *S. racemosa* and *E. acuminata* , while the older remnant trees *C. hystrix* stand out as emergent (Bhutia *et al.* , 2019; Kumar *et al.* , 2022).

2.2. Data collection

2.2.1. Sap flux measurements

Sap flux density was measured using Granier's thermal dissipation method (TDP) probes in 13 trees of the three dominant species, *S. racemosa* , *E. acuminata,* and *C. hystrix* (Granier, 1987; Lu*et al.* , 2004). The thermal dissipation method applies to a wide range of species and easy to manufacture locally at low-costs (Davis*et al.* , 2012; Flo *et al.* , 2019). The probes were installed to cover both radial and azimuthal variabilities with in an individual tree to estimate volumetric sap flow rates (V, mm h^{-1}). The detailed methodology for TDP probe manufacturing, instrumentation, and scaling to whole-tree sap flow (V in kg h^{-1}) can be referred at Kumar *et al.* (2022).

2.2.2. Scaling from whole-tree sap flow to stand transpiration

The volumetric sap flow data from the 13 trees was scaled to stand transpiration (T, mm h^{-1}) using the data from vegetation plots and sapwood area as the vegetative scalar. A five-step approach was adopted to scale

sap flow (V in kg h^{-1}) from the instrumented trees to the stand-level using tree DBH as a scalar (Chiu *et al.* , 2016). First, a non-linear least squared (NLS) regression model (intercept = 0.112, power coefficient = 0.857, $P < 0.001$) was fitted between tree diameter (DBH in m) and sapwood area (A_{total} in m^2) of the 13 trees (see supplementary data Figure S1). The NLS regression model coefficients were used to compute total sapwood are (A_{total}) from DBH for each tree (above 10 cm DBH) sampled in the vegetation plots in the next step. Third, the instrumented trees were categorized into four DBH classes < 0.15 m, 0.15-0.19 m, 0.20-0.24 m, and > 0.25 m (see supplementary data Figure S2a). The average sap flux density per class (J_{avg}) was computed by normalizing the V of each instrumented tree by its A_{total} and averaging for each class. Fourth, all trees above 10 cm DBH sampled in the vegetation plots were categorized into the above-mentioned DBH classes (see supplementary data Figure S2b). Whole-tree sap flow (V) was estimated for each tree in the forest stand by multiplying the corresponding $J_{avg}$of the diameter class with its A_{total}. Fifth, stand transpiration (T in mm h^{-1}) was computed by aggregating hourly V for all trees in the vegetation plots and dividing it by the total plot area (5000 m^2). Gap-filling of the missing data for sap flow and environmental variables was consciously avoided due to the strong variability in the raw data.

2.2.3. Environmental and hydrological measurements

An automated stilling well fitted with a capacitance water level recorder (Dataflows Systems LTD, New Zealand) was installed on the first-order stream draining the micro-watershed. Streamflow (Q, mm h^{-1}) was computed from the water-level using a stream-specific rating curve and catchment area. On-site Precipitation (P, mm h^{-1}) was recorded using an automated tipping-bucket rain gauge. Microclimate observations were used to understand the drivers of stand transpiration. Air temperature (°C), relative humidity (R_h, %), wind speed (U, m s^{-1}), and incoming short-wave radiation (R_s, kW m^{-2}) were recorded using an automatic weather station (Vantage-pro Davis Net, USA. Hourly vapour pressure deficit (D, kPa), which is an important parameter of atmospheric dryness, was computed from air temperature (°C) and relative humidity data from the weather stations and hygrochrons (iButton Hygrochrons, Maxim Int., USA). Reference evapotranspiration (E_0, mm h^{-1}) was computed the meteorological data following FAO's Penman-Monteith method (equation 6 of FAO56PM and Allen et al. 1998). Soil water potential was recorded at 10 cm incremental depths from the topsoil to up to 30 cm depth using granular matrix-based (watermark) sensors (Virtual Electronics, Roorkee) and converted to volumetric water content using the site-specific van Genuchten water retention curve developed using Rosetta software (Schaap*et al.* , 2001). Total soil moisture (S, mm) was computed for the topsoil (0-30 cm depth) using the trapezoidal method and stray missing values were gap-filled through 3-step moving-average window (Nachabe*et al.* , 2005).

2.3. Data analysis

After quality checks and clean-up, a total of 114 days (November 2013 to May 2014) of data for T, including 72 days data available for T and environmental variables (S, P, D, Q and E_0), was used for final analysis (Figure 2). The four main analytical methods used were: (a) Seasonal assessment of diurnal cycles in SPFAC variables, (b) Comparison of transpiration responses to precipitation pulses, (c) Lag correlation analysis to explore the shifting lags between Transpiration, soil moisture and streamflow, and (d) Step-wise lag regression models to quantify the relative influences of transpiration and micro-climate on streamflow. The data processing, analysis, and visualization were done in the R programming software (version 4.1.3) (R Core Team, 2022).

2.3.1. Understanding the environmental drivers of stand transpiration

Seasonal changes in diurnal cycles of sap flow and environmental drivers were plotted to illustrate the shifts in their inter-relationships. Both Q and S were de-trended to remove excessive noise (*stlplus*function, package *stlplus*) and the filtered diurnal signals, S_{diu} and Q_{diu}, respectively, were extracted for understanding diurnal patterns (Moore *et al.* , 2011). Contiguous subsets of Q longer than 5 days were subset and $Q_{daily.amp}$ was computed as the difference between highest and lowest discharge in a day for the rainless periods. The

capacitance water-level recorders used in the study are known to suffer from measurement error induced by diurnal changes in ambient temperature (Larson and Runyan, 2009). We empirically computed the measurement error (0.008 m) for the capacitance probe at the field site using a standing water column experiment with a fixed water level, and corrected for the measurement error in the estimation of $Q_{daily.amp}$. The ratio of the variance of the diurnal component of streamflow (Q_{diu}) to the variance of streamflow (Q) and the amplitude of diurnal variation in Q ($Q_{daily.amp}$) was computed for contiguous rainless periods longer than 5 days to know the seasonal variability in the significance of diurnal cycle of Q to overall Q. Hourly binned averages of P, T, $S_{diu,}$ and Q_{diu} were estimated and plotted for each month to visually assess the seasonal shifts in their respective diurnal cycles (Kumar *et al.* , 2022).

2.3.2. Impact of precipitation pulses on stand transpiration

The daily precipitation time-series was analyzed to understand the impact of precipitation pulses on plant water-use. Precipitation event volume denotes the extent of moisture input to a system and thus was preferred over intensity. Precipitation events were separated with a threshold of 2.5 mm d^{-1} and interevent time of 1-day. All events with duration longer than 2 days and total precipitation volume above 2.5 mm were considered as a pulse (Zeppel *et al.* , 2008). The percentage changes stand transpiration (T), Q, E_0, R_s and D were estimated as difference between their respective values on the day of the precipitation event and the day after (Chen *et al.* , 2014).

2.3.3. Lag correlation analysis between Transpiration, soil moisture and streamflow

Lag correlation analysis allows the quantification of correlation between variables that are at lag with each other in a physical environment and was preferred due to the observations of strong autocorrelations (Moore *et al.* , 2011; Kumar *et al.* , 2022). The lag (in hours) between following combinations: S_{diu}vs. Q_{diu}, T vs. Q_{diu} and P vs. Q_{diu} was computed for each day using the cross-correlation function (*ccf* function in R) and filtered for auto-correlation coefficients (ACF) >= |±0.4| (Moore *et al.* , 2011). Positive (negative) autocorrelation coefficient (ACF) values signified that a high (low) value of the driver variable was followed by a high (low) value of the response variable after the corresponding lag-hours (Kumar*et al.* , 2022).

2.3.4. Step-wise lag regression models for streamflow

In order to assess the relative influences of transpiration and rainfall on streamflow, a combination of a temporal lag model and the Generalized least squares (GLS) regression model (*gls* function, package*nlme*) with the suitable correlational structure were used in a step-wise manner (Kumar *et al.* , 2022). The temporal lag model was necessitated by the observed lag between the different SPFAC variables, which also showed significant temporal autocorrelations. The GLS regression method estimates the maximum likelihood of the regression coefficients using generalized least-squares and is most suitable for analyzing time-series data with autocorrelational structures (Krishnaswamy *et al.* , 2012; Kumar *et al.* , 2022). The streamflow GLS model used Q as the response variable and T, S, Antecedent moisture index (M_a), and P as predictor variables. M_a was used as a proxy for the antecedent state of moisture in the system and estimated using equation 1, where, P_{cum}, $T_{cum,}$ and Q_{cum} are cumulative sums of P, T, and Q, respectively (Potts *et al.* , 2006).

$$M_a = P_{\text{cum}} - T_{\text{cum}} - Q_{\text{cum}} \tag{1}$$

The streamflow GLS models were separately run for the rainless (December –February) and rainy (March-May) periods with first-order autoregressive structure (corAR1), which is considered suitable and parsimonious for streamflow modeling (Krishnaswamy *et al.* , 2012). The interaction term between S and T was the predictor variable in the rainless period, whereas P, M_a, and the interaction term between S and T were the predictor variables in the rainy period. Before running the models, S and M_a were normalised by subtracting the daily mean, tested for collinearity and then contiguous subsets longer than 5 days and without any missing values were extracted.

Owing to the observed lag between the driver variables, the GLS model was run using a reconstituted time-series dataset, where each driver variable was first tested for lag in a stepwise manner. For each driver variable, firstly, the highest significant lag (L in hours, at ACF >= |±0.4|) between the driver and response (Q) variable was calculated for each contiguous subset using*ccf* function. Then the driver variable was lagged from zero lag to L hours to develop multiple lagged time-series for each driver variable. Multiple linear regression models (MLRs) were fitted between Q and the lagged time-series the driver variable and the timeseries with the lowest significant lag (p [?] 0.05) was chosen. The procedure was repeated for the other driver variables and the final timeseries set was used for running the GLS model (Kumar *et al.* , 2022). We also tested for the impact of adding correlational structure to the GLS model by running the GLS model separately with and without correlations structures and comparing the results using the Analysis of variance (ANOVA) test. The GLS model with the lowest Akaike Information Criterion (AIC), higher likelihood ratio, and significance were chosen for interpretations of variables with significant coefficients (p [?] 0.05). The Gupta-Kling Efficiency (KGE) score used to assess the model performances by comparing the observed and predicted time-series of Q to (Gupta and Kling, 2011).

3. RESULTS

3.1. Stand transpiration characteristics

Average stand transpiration (T) was 1.45+-1.1 mm d^{-1}(mean+-standard deviation) approaching a maximum rate of 5.28 mm d^{-1} and ranged from 0.02-5.28 mm d^{-1}. T exceeded 3rd quartile (1.9 mm d^{-1}) of all values on 25.5 % (29 days) of the total days (114 days) of sap flow observations. The average T in summer (1.76+-1.3 mm d^{-1}) was 34 % higher than in winter (1.16+-0.8 mm d^{-1}). The nocturnal transpiration (1800 – 0500 h) was a significant fraction of (13.8 +- 6 %) of the daily T with a marginally higher proportion of evening (1800 – 0000 h) than pre-dawn flux (0000 – 0500 h). Small and medium-sized trees (DBH < 0.2 m), dominated by *S. racemosa* and *E. acuminata* , contributed to 46 % of T, whereas large-girthed trees (DBH > 0.25 m) contributed up to 40 %.

[Insert Figure 2]

Figure 2. Time-series plots of the raw daily data of the SPAC variables from winters (December) to summers (May): (a) Precipitation (P, mm d^{-1}), (b) Total Soil moisture (S, mm), (c) Stand Transpiration (T, mm d^{-1}) and (d) Streamflow (Q in mm d^{-1}).

3.2. Environmental drivers of stand transpiration

3.2.1. Shifting roles of sunlight and VPD in driving stand transpiration

R_s and D are two key drivers of transpiration when not constrained by moisture limitations. Under moisture-abundant and energy-deficient conditions, as in our case, the relative effect of R_s and D changed with season. In winter, R_s had relatively higher impact on both high and low values of T (Figure 3a), highlighted by the affinity of the scatterplot towards the x-axis. In summer, the scatter shifted to the center of the field suggesting an interactive effect of R_s and D on high values of T (Figure 3b).

[Insert Figure 3]

Figure 3. Three-dimensional scatterplot showing hourly Stand transpiration (T, z-axis) as the response variable against Incoming short-wave radiation (R_s, x-axis) and Vapour pressure deficit (D, y-axis) plotted for (a) winter and (b) summer seasons. The values are for shown for day period (0600 – 1700 h) only.

The changing dynamics can be closely observed in Figure 4, which shows continuous time-series plots of R_s, D, T, S, S_{diu}, Q, and Q_{diu} for a long rainless period in the winter. The days are consistently sunny (Figure 4a), whereas D showed strong fluctuations with initial period of high-moderate humidity followed by

atmospherically drier days (Figure 4b). In response, T was high on the initial days with high R_s and moderate D, with an unexplained spike on the day with lowest D (January 26th 2014) (Figure 4c). T increases again with another spike (4th February 2014) under high D and R_s conditions. S declined linearly over the period, whereas Q showed an abrupt decline in the middle (Figure 4d and 4f). S_{diu} had early morning troughs and afternoon peaks symptomatic of T-induced controls (Figure 4d). Conversely, Q_{diu} had bi-modal peaks in the morning and midnight, and troughs in the pre-dawn and mid-day periods (Figure 4e). In the latter half of the period, the second peak and trough smoothened out to give a unimodal pattern with a peak in the morning and trough in mid-day. The first troughs and rising limbs of S_{diu} and Q_{diu} were in sync until Q_{diu} started declining rapidly while S_{diu} declined gradually. Overall, T increased from winter to summer peaking in April.

[Insert Figure 4]

Figure 4. Time-series plots of SPAFC variables for a rainless 17-day contiguous period in winters: (a) Incoming short-wave radiation (R_s), (b) Vapour pressure deficit (D), (c) Stand transpiration (T), (d) Soil moisture (S), (f) Streamflow (Q), and (e) S_{diu} and (h) Q_{diu} are the diurnal components of soil moisture and streamflow, respectively. The vertical dashed lines mark 0000 h time for each day.

3.2.2. Impact of Precipitation pulses on Stand transpiration

A total of nine precipitation pulses were identified during the study period with total volumes ranging from 5.3–82.2 mm and mean precipitation volume of 35.9+-29.1 mm. On average, T almost doubled (93+-110 %) after the three medium-sized precipitation pulses (10-30 mm), and increased by one-third (29+-28 %) after the four large-sized pulses ([?]30 mm) (Table 1). Incidentally, the days with unusually higher values of T after the medium-sized precipitation pulse (10-30 mm) was accompanied by clear skies and high evaporative demand with increasing R_s (48+-41 %), D (14+-39 %), and E_0(51+-44 %). The days showing moderate increase in T after the four very large precipitation pulses ([?]30 mm) had proportionate increase in evaporative demand with increasing R_s (79+-45 %) and E_0 (67+-58 %), and minor reduction in D (-13+-32). Conversely, T declined significantly -64+-7% after the two small precipitation pulses (2.5-10 mm), likely due to stomatal closure caused by the significant increase in D (74+-118 %) on the following day. Expectedly, the increased in size of precipitation pulses led to exponential increase in Q, but had little effect on S.

[Insert Table 1]

Table 1. Percentage changes in transpiration and environmental variables after precipitation pulses of varying sizes (a) Incoming short-wave radiation (R_s), (b) Vapour Pressure Deficit (D), (c) Reference Evapotranspiration (E_0), (d) Stand Transpiration (T), (e) Soil moisture and (f) Streamflow (Q) (SE = standard error, N = Number of events).

3.2.3. Transpiration affecting diurnal cycles of streamflow

The seasonal changes in T are also reflected in changing diurnal cycles of S_{diu} and Q_{diu} (Supplementary Data Figure S3). The diurnal peaks in S_{diu} shifted from afternoon to evening with increasing amplitude from winter to summer. Q_{diu} showed similar patterns with increasing diurnal amplitude from the winter to summer. The summer peaks in Q_{diu} followed the afternoon peaks in P with perceptible lag. We also checked for the relative size of diurnal cycles of streamflow (Q) to the overall Q over 12 contiguous rainless periods (longer than 5 days) to understand if the diurnal cycles were significant (Figure 5). The ratio of the variance of the diurnal component of Q (Q_{diu}) to the variance of Q increased from winter to summer, peaking in March when the system was driest (Figure 5a). The low value in the April month was preceded by a large precipitation event. Similarly, the ratio of the diurnal amplitude of Q ($Q_{daily.amp}$) to daily Q (Q_{daily}) also peaked in March and November during extended rainless periods (Figure 5b).

[Insert Figure 5]

Figure 5. Barplots showing (a) mean ratio between variance of the diurnal component of streamflow (Q_{diu})

and streamflow (Q), and (b) mean ratio of the diurnal amplitude of Q ($Q_{daily.amp}$) to daily Q (Q_{daily}), computed for contiguous rainless periods in the hydrological year 2013-2014. The error bars represent standard error.

3.4. Lag correlation between Transpiration, Soil Moisture and Streamflow

The simple correlation tests between the SPAFC variables yielded low correlations due to temporal lags between the diurnal cycles of different variables. Here, the cross-correlation analysis explored the shifting lags between T, S, P and Q across distinctly separated winter (dry) and summer (wet) periods (Figure 6). T led $S_{diu}$with higher lag in winter (4.5+-4 h) with strong positive correlations (0.7+-0.1). With the advent of rains in March, T led S_{diu}than summer (1.3+-1.8 h) but with strong negative correlations (-0.8+-0.1). Similarly, in the winter, S_{diu} led Q_{diu} (2.8+-2.9 h) and with strong negative correlations (-0.7+-0.1). However, in the wet season, Q_{diu} led S_{diu} (2.8+-1 h) and strong positive correlations (0.6+-0.1). In the dry period, T led Q_{diu} (2.9+-2.5 h) and strong negative correlations (-0.7+-0.1). In the summer, the lag between T and Q_{diu} (7.4+-2.5 h) was confounded by precipitation and showed strong positive correlations (0.8+-0.1). Incidentally, T lagged Q_{diu} on certain days in winter (1.4+-0.6 h) and summer (1.3+-0.5 h) with strong negative correlations (-0.8+-0.1), which were characterized by significant pre-dawn sap flux movement (for details see Kumar *et al.* (2022)). In rainy periods, Q_{diu} lagged P (4.4+-5.4 h) strong positive correlations.

[Insert Figure 6]

Figure 6. Boxplots showing diurnal lag hours at maximum auto-correlation coefficients (ACF) for the combinations: (a) T vs. S_{diu}, (b) T vs. Q_{diu}, (c) P vs. $Q_{diu,}$ and (d) S_{diu} vs. Q_{diu},. The variables are Stand transpiration (T, mm h^{-1}), Precipitation (P, mm h^{-1}), and diurnal components of Soil moisture (S_{diu}, mm h^{-1}) and Streamflow (Q_{diu}, mm h^{-1}).

3.5. Step-wise Lag regression model for streamflow

The streamflow GLS model was fitted to four rain-free periods from November to May, including three in winter (6-17 days in length) and one in summer (27 days in length) (Table 2). The streamflow GLS model with corAR1 correlation structure had significantly lower AIC than the GLS model without any correlational structure and was chosen for model interpretation. In summer, P was lagged by an hour as per the observations of lag regression results. The streamflow GLS model showed seasonal changes in the influence of the predictors of Q with moderate concurrence ($r^2 = 0.37$, $p < 0.001$, NSE = 0.27) (Table 2). The streamflow GLS model performed better in winters with higher concurrence between predicted and observed Q ($r^2 = 0.56$, $p < 0.001$, NSE = 0.56) than summers ($r^2 = 0.31$, $p < 0.001$, NSE = 0.27). After a precipitation event, the hydrographs of predicted Q matched well with observed Q in the rising limb but failed to correspond to the falling limb (see supplementary Figure S4).

[Insert Table 2]

Table 2. Results from Generalized least squares (GLS) linear regression model with corAR1 correlational structure for streamflow (*$p< 0.05$, ** $p < 0.01$, *** $p < 0.001$). Predictor variables include Incoming shortwave radiation (R_s, kW m^{-2}), Vapour pressure deficit (D, kPa), transpiration (T, mm h^{-1}), soil moisture (S, mm h^{-1}), Precipitation (P, mm h^{-1}), Antecedent moisture index (M_a, mm h^{-1}), and the response variable is Streamflow (Q, mm h^{-1}).

At the start of the dry season, with abundant soil moisture conditions in the Event 1, the interaction term between S and T (S*T) was a moderately significant (P = 0.069) predictor of Q with negative coefficient suggesting soil moisture and transpiration are modulating streamflow in combination. As the dry season progressed, in the Event 2 ($p = 0.09$) and Event 3 ($p = 0.01$), T became the stronger predictor of Q with negative coefficients and under average S conditions. However, with the advent of precipitation in summer in the Event 4, P ($p < 0.001$) was the strongest predictor followed by M_a ($p = 0.004$), whereas the effect

of the interaction between S and T weakened considerably ($p = 0.12$). Incidentally, T had negative slope coefficients across the dry and wet periods indicating loss of potential Q to T.

4. DISCUSSION

The study site is unique in being the wettest high-elevation TMF site in the world, where direct transpiration, streamflow, and micro-climate measurements have been carried out so far (see Supplementary Figure S5) (McJannet *et al.* , 2007; Bruijnzeel *et al.* , 2011). The site falls above the 90^{th} percent quantile of the elevations and 80^{th} percent quantile of precipitation among global studies from TMFs. At the site, the low latitudinal position (27deg-28deg) and proximity to south-west Indian monsoon favor tropical climatology with the bulk of the precipitation occurring in the late-night to early morning period, a phenomenon unique to Himalaya (Barros and Lang, 2003). The studied broad-leaved montane forests in Eastern Himalaya are the most species-rich in the world and have experienced considerable human pressures (Sudhakar *et al.* , 2008; Kanade and John, 2018). The combination of high moisture availability, tropical climatology, and regenerating secondary forests provides unique conditions for observing plant-water relations and hydrological services, hitherto unstudied in the Himalaya. The study provides the first mechanistic understanding of vegetation-streamflow linkages in a very wet high elevation tropical broad-leaved evergreen wet montane forest in Eastern Himalaya. The observed vegetation-streamflow linkages are compared with results and mechanisms from other wet tropical montane forests (TMFs).

4.1. Transpiration in wet TMF of Eastern Himalaya

The rate of transpiration by a forest stand provides crucial information regarding the vegetation's capacity to recirculate moisture, which varies considerably with the age of the stand, species-specific water-use efficiency, and availability of moisture and energy. The observed mean daily transpiration (1.45+-1 mm d^{-1}) in wetter Sikkim was found to be double of the relatively drier Central Himalayan oak forests (MAP = 1331 mm) in Nepal (Ghimire *et al.* , 2014), but comparable with similarly wet low elevation (450- 650 masl) TMFs (MAP = 4200-5000 mm) in Costa Rica (Aparecido *et al.* , 2016; Moore *et al.* , 2018) and similar elevation TMF (MAP = 2067 mm) in Southern Andes (Motzer *et al.* , 2010). The maximum daily stand transpiration (5.3 mm) is 14 % higher than the highest rates (˜4.6 mm) reported from tropical montane or lowland forests (Bruijnzeel et al., 2011; McJannet et al., 2007). The observed nocturnal transpiration (T_{night}) was similar to studies (˜12 %) from China (Siddiq and Cao, 2018) and other parts of the globe (Forster, 2014). The thermal dissipation method used in the study is known to underestimate sap flow making our estimates of T conservative in nature (Flo *et al.* , 2019). The relatively higher transpiration rates, despite being at a higher elevation, possibly fueled by faster growth rates and higher interception losses from the secondary forest vegetation in a very wet environment. The high transpiration rates could also indicate evolution under the relatively wetter climate of Eastern Himalaya and merit further investigations on water-use efficiencies with changing climate (Panthi *et al.* , 2020).

Along similar lines, Pandey *et al.* (2020) have suggested that climate warming and increased summer precipitation are likely to remove moisture constraints on photosynthesis on treeline conifer and broad-leaved species in wetter parts of eastern Nepal Himalaya. This is further bolstered by faster transpiration recovery after low-mid-sized precipitation pulses. Such behaviour is usually accompanied by high evaporative demand (high E_0 and D), as seen in the Australian woodland (Burgess, 2006; Zeppel *et al.* , 2008). It is also common to forest stands with deep-rooted species as seen at the study site (Kumar *et al.* , 2022) and in the semi-arid parts of China (Chen *et al.* , 2014). The observations adds empirical evidences to the discussion on the "two worlds hypothesis" by suggesting that deep-rooted trees can access sub-surface soil moisture to fuel transpiration demands (Berry *et al.* , 2018). Here, the role of low-moderate precipitation pulses after prolonged dry period becomes crucial for the shallow-rooted pioneer species and less so for the deep-rooted late-successional species. Thus, with climate change, the predicted decline in winter precipitation and small

precipitation events may have significant impact on the structure and productivity of these regenerating secondary forests (Krishnaswamy *et al.* , 2014; Krishnan *et al.* , 2019).

4.2. Environmental driver of stand transpiration in TMFs

Similar to observations from TMFs, we observed strong seasonal fluctuations in moisture and energy conditions between winter and summer seasons (Bruijnzeel and Veneklaas, 1998; Aparecido *et al.* , 2018). The relative influence of R_s and D on T changed with season (Moore *et al.* , 2018). The observation of solar radiation driving T in winters was congruent with reports from Andes and Alps (Fiora and Cescatti, 2006; Motzer *et al.* , 2010), whereas increasing effect of D on summer T was consistent with warmer Central Himalaya (Ghimire *et al.* , 2014). Our observations of 2-3 h of lag between R_s and VPD and T were seasonally consistent and comparable with reports from TMFs in Costa Rica (Moore *et al.* , 2018) and marginally higher than reports from Tibet (˜1 hour lag) (Wang *et al.* , 2017). The lags may represent delays due to low temperature in winters and leaf wetness in the summers due to night rains or dew (Aparecido *et al.* , 2016; Moore *et al.* , 2018).

4.3. Role of transpiration in catchment ecohydrology

Few studies have explored the interactions between vegetation water use, soil moisture, and streamflow at fine temporal resolution (Moore*et al.* , 2011; Graham and Barnard, 2013). Low soil infiltration rates, as observed at the study site, coupled with high precipitation intensities may lead to higher runoff generation in the wet season. Conversely, higher moisture uptake by vegetation may lead to relatively lower streamflow output in the dry season, in comparison to a primary forest (Wright *et al.* , 2018). The GLS model results showed that, at the study site, transpiration exerted significant controls on diurnal and seasonal streamflow with soil moisture acting as the mediator in winter. T and its interaction term with S were significant predictors of Q with significant negative coefficients indicating that high T is leading to decline in Q (Bond *et al.* , 2002; Thomas *et al.* , 2012). At the study site, Kumar *et al.* , (2022) observe that the deep-rooted Fagaceae species *Castanopsis hystrix* are able to access deeper, which otherwise would have contributed to the stream as baseflow. In the summers, precipitation, and antecedent moisture (M_a) overtook as the drivers of streamflow, although the interaction term between T and S remained a significant predictor signaling continued water-uptake by vegetation.

The observed afternoon peaks in streamflow were similar to the vegetation-induced diurnal patterns in streamflow reported globally (Barnard *et al.* , 2010; Moore *et al.* , 2011; Graham and Barnard, 2013). The diurnal cycles in streamflow gained significance with the progression of dry periods and synchronized increase in vegetation activity, highlighting the controls exerted by evapotranspiration on streamflow (Bond *et al.* , 2002; Moore *et al.* , 2011). The increasing amplitudes of diurnal streamflow from winters to summers signified the growing abstraction by vegetation to support primary productivity in the dry season (Graham and Barnard, 2013; Barbeta and Penuelas, 2017). Referring back to the literature on the isotopic separation of water that contributes to transpiration and streamflow (Barbeta and Penuelas, 2017; Berry *et al.* , 2018), we suggest that in these broad-leaved Himalayan TMFs, with steep slopes and shallow soils, trees can access deeper sub-surface water for transpiration. Evidence to this are shown by Kumar *et al.* , (2022) at the study site, where groundwater is well within the reach of deep-rooted tree species like *C. hystrix*allowing them to continue transpiring at the peak of the dry season, while shallow-rooted fast-growing pioneer species like *S. racemosa* and *E. acuminata* propelled vegetation water use in moisture abundant conditions in summer. Thus, in a regenerating secondary forest, stand transpiration can have a significant impact on streamflow (Wright *et al.* , 2018) and thus, can influence diurnal precipitation patterns through active local moisture recycling, an underexplored area of investigation in vegetation-water interaction in the Himalaya (Barros and Lang, 2003).

Studies on climate change in Eastern Himalaya have predicted an increase in summer precipitation, declining winter precipitation; and increasing summer and winter temperatures (Krishnan *et al.* , 2019; Kumar*et al.* ,

2021). In summers, precipitation provides enough moisture to ensure peak vegetation productivity in April. However, increased summer precipitation in the future could result in higher cloud cover negatively impacting both vegetation productivity and transpiration leading to increased streamflow (Donohue *et al.* , 2017). The overall effect of changes in temperature and precipitation on biodiversity in the region remains complex and requires ecohydrological models specific to the East Himalayan TMFs (Asbjornsen *et al.* , 2011).

5. CONCLUSIONS

Globally, the effect of vegetation water-use on streamflow varies greatly due to species-specific, environmental and geomorphological peculiarities (Asbjornsen *et al.* , 2011; Wright *et al.* , 2018). These are the first empirical observations of mechanistic control of transpiration on streamflow under the SPAFC framework from Himalaya and add to the observations drawn by previous studies from Himalaya. Annual transpiration is double of relatively drier Central Himalaya (Ghimire *et al.* , 2014), but at the lower bound of the values reported from tropical montane cloud forests globally (Bruijnzeel*et al.* , 2011). It indicates the interactive role of precipitation and elevation in modulating the available energy, moisture, which in turn modulates the plant water-use and productivity. The time lag between streamflow and transpiration increased with seasonal dryness, until the advent of rains when precipitation was the primary driver of streamflow. Transpiration was a significant predictor of streamflow in the dry season and to a lesser extent in the wet season. The study shows that moderate precipitation pulses followed by clear skies can induce significant increase in stand transpiration. Thus, changes in vegetation cover and precipitation patterns with climate change may have a significant impact on the vegetation-streamflow linkages and local and regional moisture recycling by vegetation in the secondary broad-leaved tropical montane forests in the Eastern Himalaya. The TMFs provide protective catchments for the principal water resources, the springs, and streams, and thus better understanding their SPACF processes is critical to the quantifying ecosystem services, addressing regional water security issues and ecosystem modeling efforts. More regional studies inclusive of diurnal and seasonal variability in transpiration will be critical to increasing the accuracy of land-surface interaction models, and predicting the impact of climate change on Himalayan ecohydrology.

6. CONFLICT OF INTERESTS

The authors have no conflict of interests to declare.

7. ACKNOWLEDGMENTS

The authors are thankful to Manipal Academy of Higher Education (MAHE), Manipal, India for institutional support. The authors are grateful to the Department of Biotechnology, Govt. of India (GoI) for supporting the research through the sanctioned project titled "Technological Innovations and Ecological Research for the Sustainable Use of Bio-resources in the Eastern Himalaya" (Grant No. BT/01/NE/PS/NCBS/09). The authors thank the Department of Forests, Environment and Wildlife Management, Rural Management and Development Department, and Home Department, Govt. of Sikkim, India, and the Indian Army for research permits and field support. The study would not have been possible without the able field support from Passang Tamang, Girish Varma, Naresh Rai, the staff of Fambong-Loh Wildlife Sanctuary. The authors thank Nachiket Kelkar and Dr. Aniruddha Marathe for their useful comments on statistical analysis. The authors are indebted to Prof. Nathan G. Phillips at Boston University, USA, Prof. Frederick Meinzer at Oregon State University, USA, and Forests Science Laboratory (Corvallis), the USA for generously sharing the original thermal dissipation probe assembly design. The authors acknowledge the logistical support provided by ATREE Regional Office, Gangtok, and National Center for Biological Sciences, Bangalore, India during the study.

8. FUNDING SUPPORT

The study was funded by the Department of Biotechnology, Govt. of India (GoI) as part of the research project titled "Technological Innovations and Ecological Research for the Sustainable Use of Bio-resources in the Eastern Himalaya" (Grant No. BT/01/NE/PS/NCBS/09). The authors are also grateful to the fellowship support provided by the National Mission for Himalayan Studies (NMHS) under the Ministry of Environment, Forest and Climate Change, GoI for further fellowship support during the writing period (Grant No: GBPI/NMHS/HF/RA/2015-16/).

9. AUTHOR's CONTRIBUTIONS

Manish Kumar: Conceptualization, Methodology, Manufacturing, Testing and modification of the sap flow probes, Data collection, Formal analysis, Visualization, Writing – Original draft preparations**. Yangchenla Bhutia:** Resources, Data Curation, Writing – Review & Editing. **Gladwin Joseph:**Conceptualization, Methodology, Testing and modification of the sap flow probes, Writing – Review & Editing. **Jagdish Krishnaswamy:**Conceptualization, Methodology, Testing and modification of the sap flow probes, Writing – Review & Editing, Supervision, Project Administration, Funding acquisition.

10. DATA SHARING

The data that support the findings of this study are available on request from the corresponding author. The data are not publicly available due to privacy or ethical restrictions. A sample subset of the data that support the findings of this study is available in Dryad at https://doi.org/10.5061/dryad.47d7wm3cg under the citation Kumar (2021). The sample dataset is available for preview at the following url:

https://datadryad.org/stash/share/bkDWLqnM4S2C3w0wgri1AcXlyDz3eM2Sgs7prOqLZqk

11. REFERENCES

Allen RG, Pereira LS, Raes D, Smith M. 1998. Crop evapotranspiration: Guidelines for computing crop requirements. *Irrigation and Drainage Paper No. 56, FAO* (56): 300 DOI: 10.1016/j.eja.2010.12.001

Aparecido LMT, Miller GR, Cahill AT, Moore GW. 2016. Comparison of tree transpiration under wet and dry canopy conditions in a Costa Rican premontane tropical forest. *Hydrological Processes* **30**(26): 5000–5011 DOI: 10.1002/hyp.10960

Aparecido LMT, Teodoro GS, Mosquera G, Brum M, Barros F de V., Pompeu PV, Rodas M, Lazo P, Muller CS, Mulligan M, et al. 2018. Ecohydrological drivers of Neotropical vegetation in montane ecosystems.*Ecohydrology* **11** (3) DOI: 10.1002/eco.1932

Asbjornsen H, Goldsmith GR, Alvarado-Barrientos MS, Rebel K, Van Osch FP, Rietkerk M, Chen J, Gotsch S, Tobon C, Geissert DR, et al. 2011. Ecohydrological advances and applications in plant-water relations research: A review. *Journal of Plant Ecology* **4** (1–2): 3–22 DOI: 10.1093/jpe/rtr005

Barbeta A, Penuelas J. 2017. Relative contribution of groundwater to plant transpiration estimated with stable isotopes. *Scientific Reports* **7** (1): 1–10 DOI: 10.1038/s41598-017-09643-x

Barnard HR, Graham CB, Van Verseveld WJ, Brooks JR, Bond, B. J. &, McDonnell JJ. 2010. Mechanistic assessment of hillslope transpiration controls of diel subsurface flow: a steady-state irrigation approach.*Ecohydrology* **130** (February): 126–130 DOI: 10.1002/eco

Barros AP, Lang TJ. 2003. Monitoring the Monsoon in the Himalayas: Observations in Central Nepal, June 2001. *Monthly Weather Review***131** (7): 1408–1427 DOI: 10.1175/1520-0493(2003)131<1408:MTMITH>2.0.CO;2

Berry ZC, Evaristo J, Moore G, Poca M, Steppe K, Verrot L, Asbjornsen H, Borma LS, Bretfeld M, Herve-Fernandez P, et al. 2018. The two water worlds hypothesis: Addressing multiple working hypotheses and proposing a way forward. *Ecohydrology* **11** (3) DOI: 10.1002/eco.1843

Bhutia Y, Gudasalamani R, Ganesan R, Saha S. 2019. Assessing forest structure and composition along the altitudinal gradient in the state of Sikkim, Eastern Himalayas, India. *Forests* **10** (8): 1–17 DOI: 10.3390/f10080633

Bond BJ, Jones J a., Moore G, Phillips N, Post D, McDonnell JJ. 2002. The zone of vegetation influence on baseflow revealed by diel patterns of streamflow and vegetation water use in a headwater basin.*Hydrological Processes* **16** (8): 1671–1677 DOI: 10.1002/hyp.5022

Bruijnzeel L. 2004. *Hydrological functions of tropical forests: not seeing the soil for the trees?* DOI: 10.1016/j.agee.2004.01.015

Bruijnzeel LA, Veneklaas EJ. 1998. Climatic conditions and tropical montane forest productivity: The fog has not lifted yet. *Ecology***79** (1): 3–9 DOI: 10.1890/0012-9658(1998)079[0003:CCATMF]2.0.CO;2

Bruijnzeel LA, Mulligan M, Scatena FN. 2011. Hydrometeorology of tropical montane cloud forests: Emerging patterns. *Hydrological Processes* **25** (3): 465–498 DOI: 10.1002/hyp.7974

Burgess SSO. 2006. Measuring transpiration responses to summer precipitation in a Mediterranean climate: A simple screening tool for identifying plant water-use strategies. *Physiologia Plantarum***127** (3): 404–412 DOI: 10.1111/j.1399-3054.2006.00669.x

Celleri R, Feyen J. 2009. The Hydrology of Tropical Andean Ecosystems: Importance, Knowledge Status, and Perspectives. *Mountain Research and Development* **29** (4): 350–355 DOI: 10.1659/mrd.00007

Chen L, Zhang Z, Zeppel M, Liu C, Guo J, Zhu J, Zhang X, Zhang J, Zha T. 2014. Response of transpiration to rain pulses for two tree species in a semiarid plantation. *International journal of biometeorology***58** (7): 1569–1581 DOI: 10.1007/s00484-013-0761-9

Chiu CW, Komatsu H, Katayama A, Otsuki K. 2016. Scaling-up from tree to stand transpiration for a warm-temperate multi-specific broadleaved forest with a wide variation in stem diameter. *Journal of Forest Research* **21** (4): 161–169 DOI: 10.1007/s10310-016-0532-7

Davis TW, Kuo C-M, Liang X, Yu P-S. 2012. Sap flow sensors: construction, quality control and comparison. *Sensors (Basel, Switzerland)* **12** (1): 954–71 DOI: 10.3390/s120100954

Deng Y, Wu S, Ke J, Zhu A. 2021. Effects of meteorological factors and groundwater depths on plant sap flow velocities in karst critical zone.*Science of the Total Environment* **781** (50): 146764 DOI: 10.1016/j.scitotenv.2021.146764

Donohue RJ, Roderick ML, McVicar TR, Yang Y. 2017. A simple hypothesis of how leaf and canopy-level transpiration and assimilation respond to elevated CO2 reveals distinct response patterns between disturbed and undisturbed vegetation. *Journal of Geophysical Research: Biogeosciences* **122** (1): 168–184 DOI: 10.1002/2016JG003505

Fiora A, Cescatti A. 2006. Diurnal and seasonal variability in radial distribution of sap flux density: Implications for estimating stand transpiration. *Tree Physiology* **26** (9): 1217–1225 DOI: 10.1093/treephys/26.9.1217

Flo V, Martinez-Vilalta J, Steppe K, Schuldt B, Poyatos R. 2019. A synthesis of bias and uncertainty in sap flow methods.*Agricultural and Forest Meteorology* **271** (March): 362–374 DOI: 10.1016/j.agrformet.2019.03.012

Forster MA. 2014. How significant is nocturnal sap flow? *Tree Physiology* **34** (7): 757–765 DOI: 10.1093/treephys/tpu051

Ghimire CP, Lubczynski MW, Bruijnzeel LA, Chavarro-Rincon D. 2014. Transpiration and canopy conductance of two contrasting forest types in the Lesser Himalaya of Central Nepal. *Agricultural and Forest Meteorology* **197** : 76–90 DOI: 10.1016/j.agrformet.2014.05.012

Graham C, Barnard H. 2013. Catchment scale controls the temporal connection of transpiration and diel fluctuations in streamflow.*Hydrological ...* DOI: 10.1002/hyp

Granier A. 1987. Evaluation of transpiration in a Douglas-fir stand by means of sap flow measurements. *Tree physiology* **3** (4): 309–20 Available at: http://www.ncbi.nlm.nih.gov/pubmed/14975915

Gupta HV, Kling H. 2011. On typical range, sensitivity, and normalization of Mean Squared Error and Nash-Sutcliffe Efficiency type metrics. *Water Resources Research* **47** (10): 2–4 DOI: 10.1029/2011WR010962

Kanade R, John R. 2018. Topographical influence on recent deforestation and degradation in the Sikkim Himalaya in India; Implications for conservation of East Himalayan broadleaf forest. *Applied Geography* **92** : 85–93 DOI: 10.1016/j.apgeog.2018.02.004

Krishnan R, Shrestha AB, Ren G, Rajbhandari R, Saeed S, Sanjay J, Syed A, Vellore R, Xu Y, You Q, et al. 2019. Unravelling Climate Change in the Hindu Kush Himalaya: Rapid Warming in the Mountains and Increasing Extremes. In *The Hindu Kush Himalaya Assessment* , Wester P, , Mishra A, , Mukherji A, , Shrestha AB, , Change C (eds).Springer International Publishing. DOI: 10.1007/978-3-319-92288-1

Krishnaswamy J. 2017. Forest Management and Water in India. In*Forest Management and the Impact on Water Resources: A Review of 13 Countries* , Garcia Chevesich P, , Neary DG, , Scott DF, , Benyon RG, , Reyna T (eds).UNESCO Publishing; 87–104.

Krishnaswamy J, Bonell M, Venkatesh B, Purandara BK, Lele S, Kiran MC, Reddy V, Badiger S, Rakesh KN. 2012. The rain-runoff response of tropical humid forest ecosystems to use and reforestation in the western ghats of India. *Journal of Hydrology* **472** –**473** : 216–237 DOI: 10.1016/j.jhydrol.2012.09.016

Krishnaswamy J, Bonell M, Venkatesh B, Purandara BK, Rakesh KN, Lele S, Kiran MC, Reddy V, Badiger S. 2013. The groundwater recharge response and hydrologic services of tropical humid forest ecosystems to use and reforestation: Support for the 'infiltration-evapotranspiration trade-off hypothesis'. *Journal of Hydrology* **498** : 191–209 DOI: 10.1016/j.jhydrol.2013.06.034

Krishnaswamy J, John R, Joseph S. 2014. Consistent response of vegetation dynamics to recent climate change in tropical mountain regions. *Global Change Biology* **20** (1): 203–215 DOI: 10.1111/gcb.12362

Kumar M, Bhutia Y, Joseph G, Krishnaswamy J. 2022. Differential water-use strategies in co-occurring pioneers and late-successional tree species in secondary tropical montane forests of Eastern Himalaya.

Preprint

Kumar M, Hodnebrog O, Sophie Daloz A, Sen S, Badiger S, Krishnaswamy J. 2021. Measuring precipitation in Eastern Himalaya: Ground validation of eleven satellite, model and gauge interpolated gridded products.*Journal of Hydrology* **599** DOI: 10.1016/j.jhydrol.2021.126252

Larson P, Runyan C. 2009. Evaluation of a Capacitance Water Level Recorder and Calibration Methods in an Urban Environment. *CUERE Technical Memo* (September): 36 Available at: http://www.umbc.edu/cuere/BaltimoreWTB/pdf/TM_2009_003.pdf

Lu P, Urban L, Ping Z. 2004. Granier's Thermal Dissipation Probe (TDP) Method for Measuring Sap Flow in Trees : Theory and Practice.*Acta Botanica Sinica* **46** (6): 631–646

Maeght J, Rewald B, Pierret A. 2013. How to study deep roots—and why it matters. *Frontiers in Plant Science* **4** (August): 1–14 DOI: 10.3389/fpls.2013.00299

McJannet, D., Fitch P, Disher M, Wallace J. 2007. Measurements of transpiration in four tropical rainforest types of north Queensland, Australia. *Hydrological Processes* **21** (July): 3549–3564 DOI: 10.1002/hyp

Moore GW, Jones JA, Bond BJ. 2011. How soil moisture mediates the influence of transpiration on streamflow at hourly to interannual scales in a forested catchment. *Hydrological Processes* **25** (24): 3701–3710 DOI: 10.1002/hyp.8095

Moore GW, Orozco G, Aparecido LMT, Miller GR. 2018. Upscaling transpiration in diverse forests: Insights from a tropical premontane site. *Ecohydrology* **11** (3): 1–13 DOI: 10.1002/eco.1920

Motzer T, Munz N, Anhuf D, Kuppers M. 2010. Transpiration and microclimate of a tropical montane rain forest, southern Ecuador. In *Tropical Montane Cloud Forests: Science for Conservation and Management* , Bruijnzeel L. A., Scatena F. N. HLS (ed.).Cambridge University Press; 447–455. DOI: 10.1017/CBO9780511778384.049

Nachabe M, Shah N, Ross M, Vomacka J. 2005. Evapotranspiration of Two Vegetation Covers in a Shallow Water Table Environment. *Soil Science Society of America Journal* **69** (2): 492 DOI: 10.2136/sssaj2005.0492

Pandey PK, Dabral PP, Pandey V. 2016. Evaluation of reference evapotranspiration methods for the northeastern region of India.*International Soil and Water Conservation Research* **4**(1): 52–63 DOI: 10.1016/j.iswcr.2016.02.003

Pandey S, Cherubini P, Saurer M, Carrer M, Petit G. 2020. Effects of climate change on treeline trees in Sagarmatha (Mt. Everest, Central Himalaya). *Journal of Vegetation Science* **31** (6): 1146–1155 DOI: 10.1111/jvs.12921

Panthi S, Fan ZX, van der Sleen P, Zuidema PA. 2020. Long-term physiological and growth responses of Himalayan fir to environmental change are mediated by mean climate. *Global Change Biology***26** (3): 1778–1794 DOI: 10.1111/gcb.14910

Pavlis J, Jenik J. 2000. Roots of pioneer trees in amazonian rain forest. *Trees - Structure and Function* **14** (8): 442–455 DOI: 10.1007/s004680000049

Pena-Arancibia JL, Bruijnzeel LA, Mulligan M, van Dijk AIJM. 2019. Forests as 'sponges' and 'pumps': Assessing the impact of deforestation on dry-season flows across the tropics. *Journal of Hydrology***574** : 946–963 DOI: 10.1016/j.jhydrol.2019.04.064

Perry TD, Jones JA. 2017. Summer streamflow deficits from regenerating Douglas-fir forest in the Pacific Northwest, USA. *Ecohydrology***10** (2): 1–13 DOI: 10.1002/eco.1790

Potts DL, Huxman TE, Cable JM, English NB, Ignace DD, Eilts JA, Mason MJ, Weltzin JF, Williams DG. 2006. Antecedent moisture and seasonal precipitation influence the response of canopy-scale carbon and water exchange to rainfall pulses in a semi-arid grassland. *New Phytologist* **170** (4): 849–860 DOI: 10.1111/j.1469-8137.2006.01732.x

Qazi NQ, Bruijnzeel LA, Rai SP, Ghimire CP. 2017. Impact of forest degradation on streamflow regime and runoff response to rainfall in the Garhwal Himalaya, Northwest India. *Hydrological Sciences Journal***62** (7): 1114–1130 DOI: 10.1080/02626667.2017.1308637

R Core Team. 2022. R: A language and environment for statistical computing. R Foundation for Statistical Computing, Vienna, Austria. DOI: 10.1108/eb003648

Schaap MG, Leij FJ, Van Genuchten MT. 2001. Rosetta: A computer program for estimating soil hydraulic parameters with hierarchical pedotransfer functions. *Journal of Hydrology* **251** (3–4): 163–176 DOI: 10.1016/S0022-1694(01)00466-8

Schlesinger W, Jasechko S. 2014. Transpiration in the global water cycle. *Agricultural and Forest Meteorology***189** –**190** : 115–117

Sharma E, Bhuchar S, Xing MA, Kothyari BP. 2007. Land use change and its impact on hydro-ecological linkages in Himalayan watersheds. *Tropical Ecology* **48** (2): 151–161

Siddiq Z, Cao KF. 2018. Nocturnal transpiration in 18 broadleaf timber species under a tropical seasonal climate. *Forest Ecology and Management* **418** (October): 47–54 DOI: 10.1016/j.foreco.2017.12.043

Singh P, Bengtsson L. 2005. Impact of warmer climate on melt and evaporation for the rainfed, snowfed and glacierfed basins in the Himalayan region. *Journal of Hydrology* **300** (1–4): 140–154 DOI: 10.1016/j.jhydrol.2004.06.005

Singh P, Kumar A. 2010. Hydro-meteorological correlations and relationships for estimating stream flow for Gangotri Glacier basin in Western Himalayas. *International Journal of ...* **2**(3): 60–69 Available at: http://www.academicjournals.org/IJWREE/PDF/pdf 2010/May/Singh et al.pdf [Accessed 25 May 2013]

Sudhakar S, Prasad PRC, Arrawatia ML, Sudha K, Babar S, Rajeshwar Rao SKSV. 2008. Landscape analysis in Fambong Lho wildlife sanctuary, east district, Sikkim, India using remote sensing and GIS techniques. *Journal of the Indian Society of Remote Sensing* **36** (2): 203–216 DOI: 10.1007/s12524-008-0021-3

Thomas Z, Ghazavi R, Merot P, Granier A. 2012. Modelling and observation of hedgerow transpiration effect on water balance components at the hillslope scale in Brittany. *Hydrological Processes* **26**(26): 4001–4014 DOI: 10.1002/hyp.9198

Wang H, He K, Li R, Sheng Z, Tian Y, Wen J, Chang B. 2017. Impact of time lags on diurnal estimates of canopy transpiration and canopy conductance from sap-flow measurements of Populus cathayana in the Qinghai–Tibetan Plateau. *Journal of Forestry Research* **28** (3): 481–490 DOI: 10.1007/s11676-016-0333-z

Wohl E, Barros A, Brunsell N, Chappell NA, Coe M, Giambelluca T, Goldsmith S, Harmon R, Hendrickx JMH, Juvik J, et al. 2012. The hydrology of the humid tropics. *Nature Climate Change* **2**(9): 655–662 DOI: 10.1038/nclimate1556

Wright C, Kagawa-Viviani A, Gerlein-Safdi C, Mosquera GM, Poca M, Tseng H, Chun KP. 2018. Advancing ecohydrology in the changing tropics: Perspectives from early career scientists. *Ecohydrology* **11** (3): 1–18 DOI: 10.1002/eco.1918

Zeppel M, Macinnis-Ng CMO, Ford CR, Eamus D. 2008. The response of sap flow to pulses of rain in a temperate Australian woodland. *Plant and Soil* **305** (1–2): 121–130 DOI: 10.1007/s11104-007-9349-7

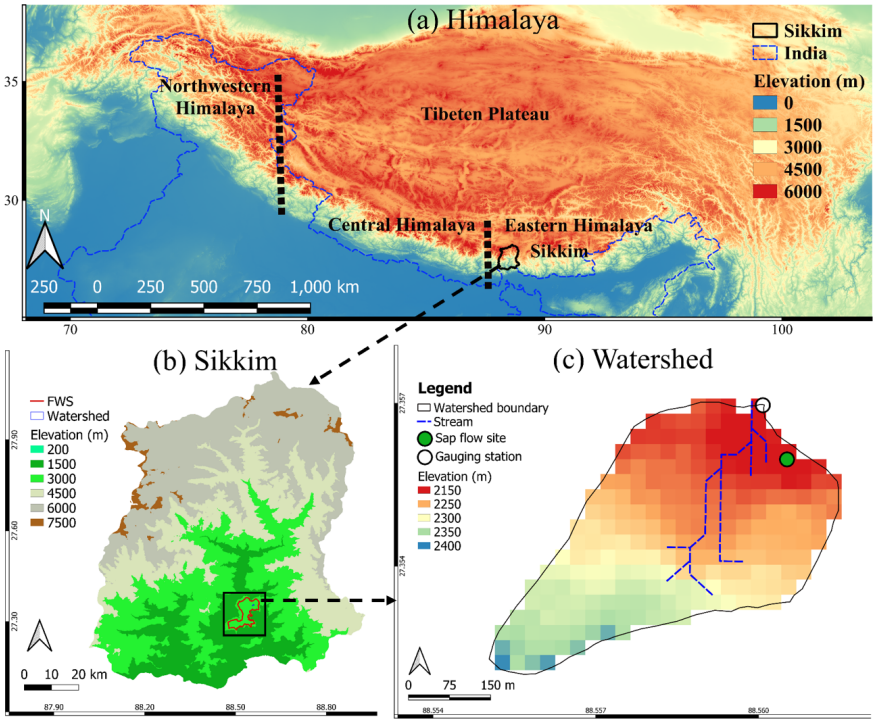

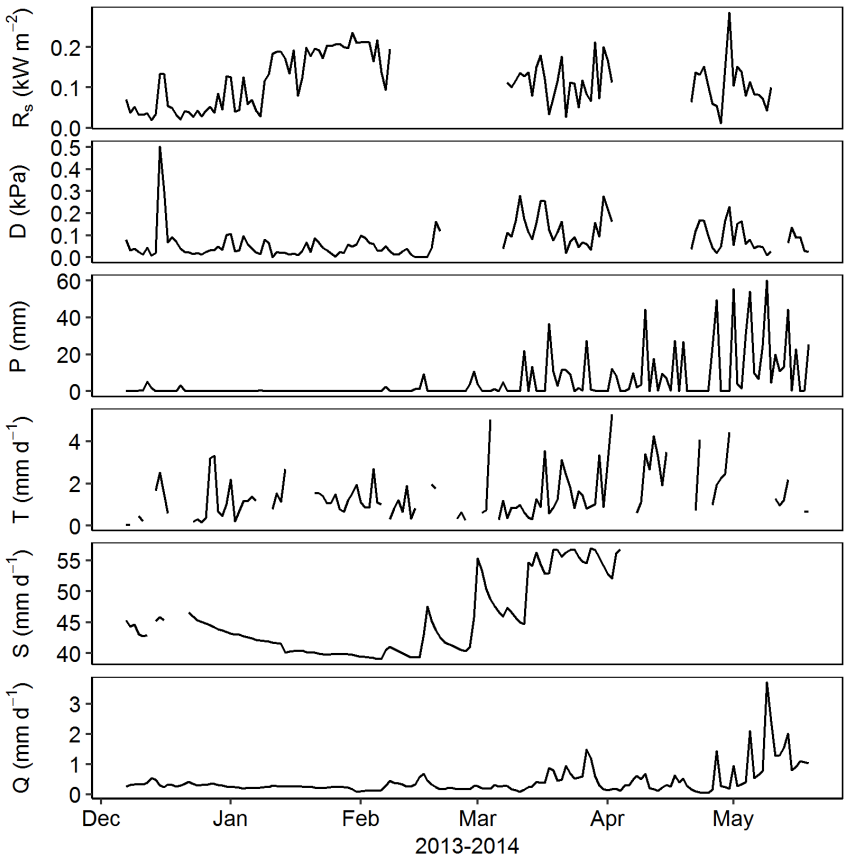

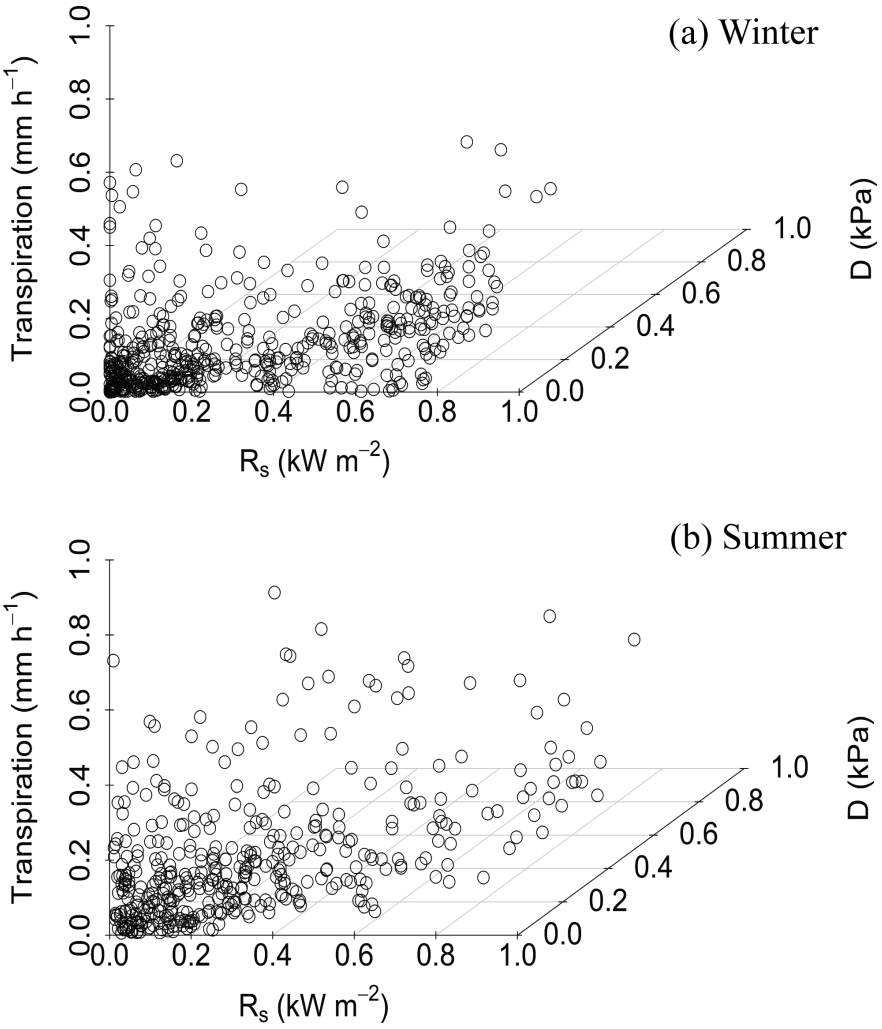

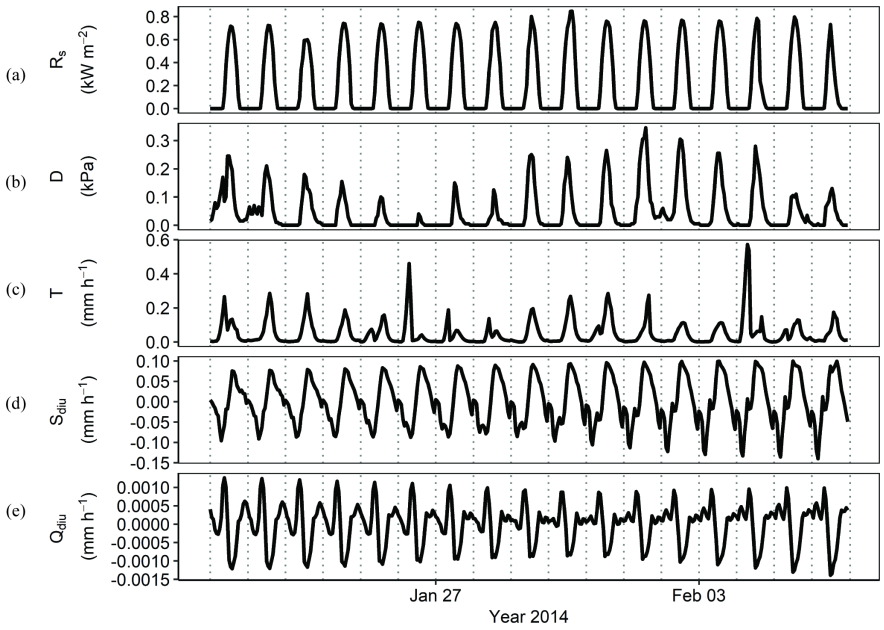

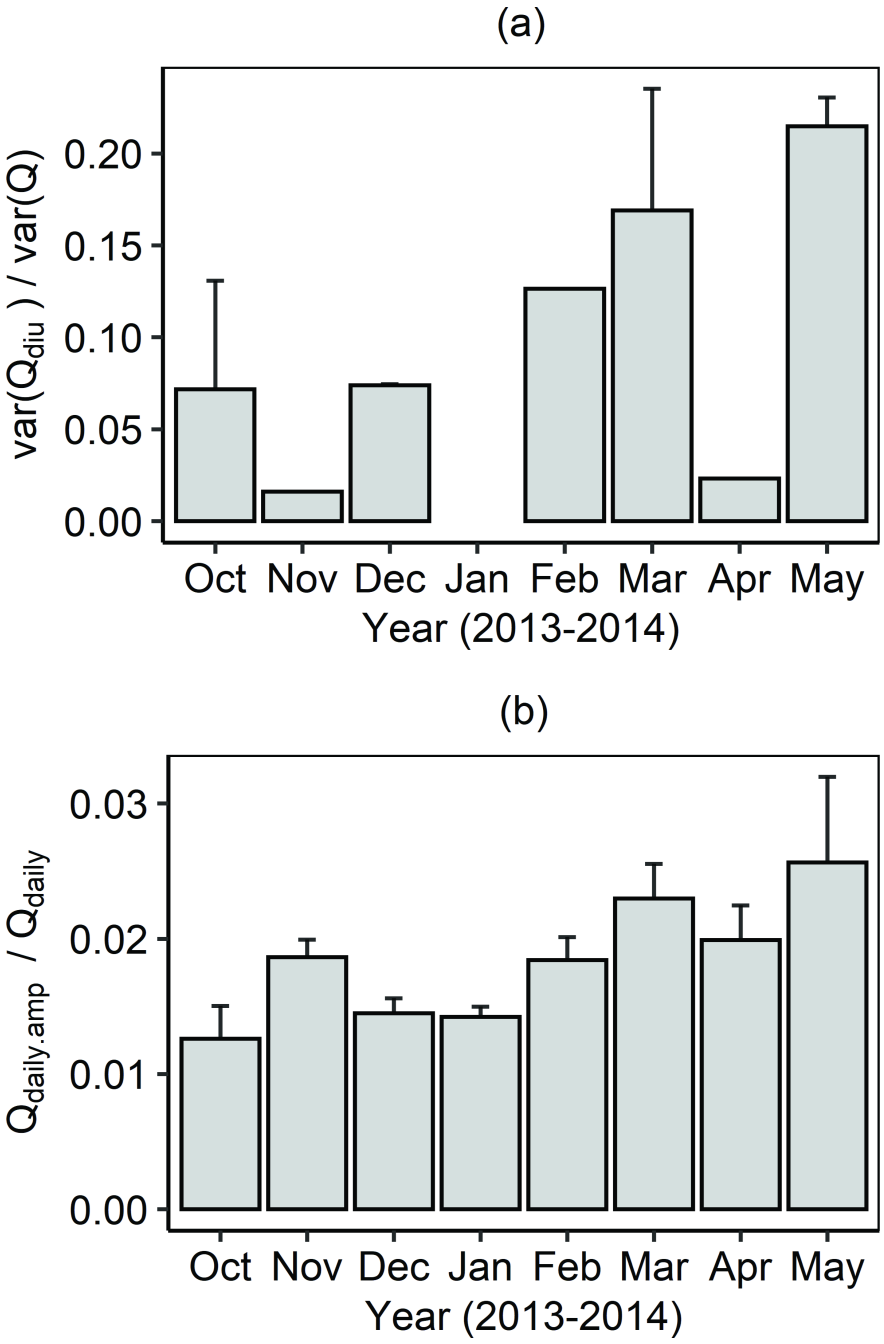

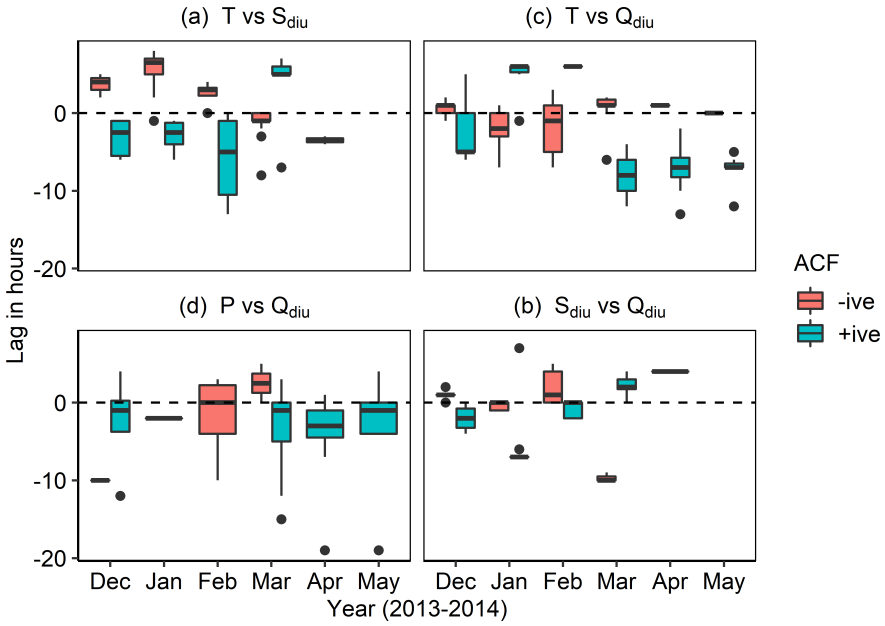

Hosted file

Table 1.docx available at https://authorea.com/users/564463/articles/611257-transpiration-drives-diurnal-and-seasonal-streamflow-in-secondary-tropical-montane-forests-of-eastern-himalaya

Hosted file

Table 2.docx available at https://authorea.com/users/564463/articles/611257-transpiration-drives-diurnal-and-seasonal-streamflow-in-secondary-tropical-montane-forests-of-eastern-himalaya